

Therapeutic efficacy of *Trichinella spiralis* nano-cathepsin B antigen in murine trichinosis

Original
Article

Amany F Atia, Wafaa M El-Kersh, Nadia S El-Nahas, Ismail M Moharm, Marwa E Lasheen, Noha M Abo-Hussien

Department of Parasitology, Faculty of Medicine, Menoufia University

ABSTRACT

Background: The conventional anti-helminthic treatment for trichinosis has limited efficacy against encapsulated muscle larvae of *T. spiralis*. An efficient therapeutic formula is needed to terminate the encapsulated forms.

Objective: To study the therapeutic efficacy of the highly antigenic *T. spiralis* cathepsin B (TsCB) and TsCB loaded on nanoliposomes drug delivery system, as an efficient drug delivery system system, with/without aluminum hydroxide as adjuvant in murine trichinosis.

Material and Methods: Seventy male Swiss albino mice were divided into two groups: control (non-infected and *T. spiralis*-infected subgroups), and treated groups. Compared to Albendazole treated group, mice of the treated group were divided into four other subgroups according to therapeutic regimens. To study the therapeutic efficacy in intestinal, and muscular phases, half of the mice in each infected subgroup were sacrificed on the 7th day post-infection (dpi), and the other half on the 35th dpi to count *T. spiralis* adults and larvae, and to examine the histopathological changes. Quantitative levels of IgM, IgG1, and *T. spiralis* circulating larval antigen were determined by ELISA. Real-time PCR was used for the detection of *T. spiralis* larval DNA in the intestinal and the muscular tissues.

Results: The treated groups showed a reduction in adult and larval counts and an improvement in inflammation with minimal eosinophilic infiltrate. Moreover, increased optical density (OD) of serum IgM and IgG1, decreased *Trichinella* circulating antigen levels, and increased mean cycle threshold of *T. spiralis* larva DNA were recorded. The best results of all parameters were detected in mice treated by nano-CB with aluminum hydroxide.

Conclusion: It was concluded that CB, and nanoliposomes CB have high therapeutic effects on experimental trichinosis, and aluminum hydroxide improves the efficacy of each.

Keywords: albendazole; aluminum hydroxide; cathepsin B; circulating larval antigen, IgG1, IgM, nanoliposomes, real time PCR; trichinosis.

Received: 5 October, 2023; **Accepted:** 24 November, 2023.

Corresponding Author: Marwa E. Lasheen; **Tel.:** +20 1113541519; **Email:** marwalasheen71@gmail.com

Print ISSN: 1687-7942, **Online ISSN:** 2090-2646, **Vol. 16, No. 3, December, 2023.**

INTRODUCTION

Trichinosis is a parasitic infection caused by *T. spiralis*, resulting in serious parasitic zoonosis and a globally endemic disease^[1]. Humans acquire the infection by ingestion of uncooked or inadequately cooked meat contaminated with *T. spiralis* larvae. Upon ingestion, the larvae are freed from their capsules and invade the upper small intestine's epithelial cells, where they develop into adult worms. The fertilized females give birth to around 1500 newborn larvae in two to three weeks, which infiltrate through the blood and lymphatic systems to encapsulate in the skeletal muscles^[2].

The conventional anti-helminthic treatment, such as albendazole, exhibited poor absorption and acquired resistance, which reduced its effectiveness against encapsulated muscle larvae. Additionally, it should not be used by pregnant women or infants^[3]. Thus, there is a critical demand for anti-*Trichinella* medications that are secure, efficient, and less harmful.

Cysteine protease enzymes are expressed by all eukaryotes. In many cases, their secretion has a vital function in the host-parasite relationship. They play essential role(s) in parasite penetration, migration, molting, and immune escaping. Parasite secreted CB is directly exposed to the host immune system. Therefore, it is highly antigenic and appears to be a potential vaccine target^[4]. Moreover, excretory/secretory (E/S) products or somatic proteins of *T. spiralis* were found to promote larvae penetration of intestinal epithelial cells in the process of *Trichinella* infection, which is the most needed step^[5]. In addition, *T. spiralis* infected mice develop a Th2 response after receiving treatment with recombinant TsCB^[6].

Recent developments in disease detection, treatment formulation and delivery, all depend greatly on nanotechnology^[7]. Chosen nanocarriers for use in medical applications must be both nontoxic (harmless to a given biological system) and biocompatible (able to integrate with a biological system without evoking an immune response or any negative effects). Therapeutic

agents are released after the drug-nanocarrier conjugates reach the diseased tissues. Drugs can be released from nanocarriers in a regulated manner^[8].

Nanoliposomes have several uses in the pharmaceutical and cosmetics sectors. They can save delicate materials from damage, enable the combination of several elements, and stop unpleasant flavors from interacting with taste receptors. A controlled release system of nanoliposomes enables the addition of substances like enzymes or antibacterial agents before their action time without causing bad consequences^[9]. Additionally, due to their advantages, nanoliposomes are used in biomedical applications as an efficient drug delivery system^[10]. Liposomes are powerful immune adjuvants for promoting humoral and/or cellular immune responses without causing hypersensitive reactions. The immune response can be affected by the liposome bilayer's fluidity^[11].

Moreover, adjuvants that are frequently employed in several vaccination systems can modulate cellular and humoral immune responses without causing local or widespread reactions. In a murine model of trichinosis, aluminum hydroxide was utilized to emulsify several antigens to test the effectiveness of their protective immunity against trichinosis. It acts through promoting the secretion of Th2 type cytokines from a variety of receptors and ligands in the hosts, which encourage mast cell activation and hyperplasia, both of which are necessary for worm release and intestinal epithelial cell permeability^[12]. Antibodies (IgG, IgM, and IgA) have a significant role against trichinosis by entrapment and rapid expulsion of infective first-stage rhabditiform

larvae (L1 larvae), reducing adult worm fecundity and participating in the killing of newborn larvae^[13].

The present work aimed to study the therapeutic efficacy of *TsCB* alone and carried on nanoliposomes with and without aluminum hydroxide as an adjuvant in murine trichinosis.

MATERIAL AND METHODS

This experimental case-control study was conducted at Theodore Bilharz Research Institute (TBRI), Giza, Egypt, and Pathology Department, Faculty of Medicine, Menoufia University, Shebeen El-Koum, Egypt during the period from March 2020 to April 2021.

Study design: Mice were classified into two groups; group I (two control subgroups), and group II (five treated subgroups). Mice of all groups were equally sacrificed on the 7th day dpi and the 35th dpi to evaluate *TsCB* efficacy during intestinal and muscular phases, respectively. Evaluation parameters employed included parasitological, histopathological, immunological, and molecular studies.

Experimental animals: Seventy Swiss male albino mice (~eight weeks old and 25±0.2 gram) bred at TBRI, were maintained according to the National Guidelines for Experimental Animal Welfare.

Drugs and chemicals: Table (1) shows drugs and chemicals used in the study.

Table 1. Drugs and chemicals used in the study.

Methods	Drugs/chemicals	Company/Country of manufacture
Preparatory methods	Liposome nanoparticles	Nano Tech, Egypt
	Albendazole suspension	Egyptian International Pharmaceutical Industries company
Serum IgM and IgG1	Maxsorp 96-well micro-titre plates	Nunc, Denmark
	Carbonate-bicarbonate buffer	Sigma, UK
	Bovine serum albumin	Sigma-Aldrich, UK
	Tween 20	Sigma-Aldrich, UK
	Anti-mouse IgM and IgG	Southern Biotech, USA
	Pnitrophenyl phosphate substrate	Sigma-Aldrich, UK
Real-time PCR	JET™ Genomic DNA purification mini-kit	Thermo Scientific, EU/Lithuania
	Taq DNA polymerase	Genecraft, Germany
	dNTPS	Stratagene, USA
	Primers	Midland, Texas
	SYBR® Green	Quantace Ltd.

Study groups: Table (2) demonstrates the characteristics of each group and subgroup, and time of sacrifice.

Mice infection: *T. spiralis* strain was kindly obtained from Medical Parasitology Department, Tanta University, Egypt. The European Union Reference Laboratory for Parasites previously genotyped this strain that was maintained in the Parasitology

laboratory of Tanta University by repeated passages through rats and mice. Mice were given 300 *T. spiralis* larvae per mouse for oral infection^[14].

Preparation of *T. spiralis* CB (*TsCB*): Adult *T. spiralis* were allocated in 1 ml phosphate buffered saline (PBS) and homogenized at 1500 rpm for 10 min at 4°C, then diluted with 3 ml PBS to obtain the crude antigen. To isolate *TsCB*, the crude antigen was purified

Table 2. Characteristics of the study groups and subgroups.

Groups	No.	Characteristics
Group I: Control group	20	
Ia: Control negative Included 2 subgroups (5 mice each)	10 5	Not infected, not treated: Each mouse received 0.2 ml physiological saline.
	5	Ia1: Scarified on 7 th dpi to assess intestinal phase.
	5	Ia2: Scarified on 35 th dpi to assess muscular phase.
Ib: Control positive Included 2 subgroups (5 mice each)	10 5	Infected not treated: Each mouse received 300 <i>Trichinella</i> larvae infection orally
	5	Ib1: Scarified on 7 th dpi to assess intestinal phase.
	5	Ib2: Scarified on 35 th dpi to assess muscular phase.
Group II: Treated group	50	Mice were infected orally by 300 <i>T. spiralis</i> larvae then treated by a different material according to subgroup.
Subgroup IIa: CB Included 2 subgroups (5 mice each)	10 5	Treated with CB
	5	IIa1: Scarified on 7 th dpi to assess intestinal phase.
	5	IIa2: Scarified on 35 th dpi to assess muscular phase.
Subgroup IIb: Nano-CB Included 2 subgroups (5 mice each)	10 5	Treated with CB carried on nanoliposomes
	5	IIb1: Scarified on 7 th dpi to assess intestinal phase.
	5	IIb2: Scarified on 35 th dpi to assess muscular phase.
Subgroup IIc: CB + adjuvant Included 2 subgroups (5 mice each)	10 5	Treated with CB and aluminum hydroxide adjuvant
	5	IIc1: Scarified on 7 th dpi to assess intestinal phase.
	5	IIc2: Scarified on 35 th dpi to assess muscular phase.
Subgroup IId: Nano-CB + adjuvant Included 2 subgroups (5 mice each)	10 5	Treated with CB carried on nanoliposomes, and aluminum hydroxide
	5	IId1: Scarified on 7 th dpi to assess intestinal phase.
	5	IId2: Scarified on 35 th dpi to assess muscular phase.
Subgroup IIe: Albendazole Included 2 subgroups (5 mice each)	10 5	Treated with Albendazole
	5	IIe1: Scarified on 7 th dpi to assess intestinal phase.
	5	IIe2: Scarified on 35 th dpi to assess muscular phase.

by two methods: ion exchange chromatography method using diethyl amino-ethyl-cellulose (DEAE) (sephadex chromatography A-50), and gel filtration chromatography method using Sephadex-G-200 HR column^[15]. Protein content was adjusted (5 µg/ml) in PBS. Part of the pure TsCB was conjugated later with nanoliposomes.

Preparation of nano-CB: Liposome nanoparticles were synthesized according to conventional wet chemical procedures, in which 150 ml of liposome nanoparticles were incubated with 600 µg CB. Then, the conjugates were ultra-centrifuged at 2500 rpm at 10°C for one h^[16].

Drug regimens

- **CB and CB-nanoliposome** were used in a dose of 25 µg each, for intraperitoneal injection^[6] for six days from the first day of infection^[17]. Each mouse was injected with 5 ml/dose of the prepared protein in PBS.
- **Aluminum hydroxide:** It was kindly obtained from TBRI, and was prepared according to Lindblad^[18]. It was used as adjuvant at 1.2 mg/dose in subgroups IIc (TsCP), and IId (nanoliposomes-TsCB). Its optimal adjuvanticity was obtained at a concentration of 2%.
- **Albendazole suspension** (20 mg/ml) was given orally in a dose 50 mg/kg/day for three successive days starting from the 1st day of infection^[19]. Each mouse (~25 g) was administered 0.25 ml/day.

Tissue specimens' collection: Mice of all groups were euthanized by cervical dislocation on the 7th dpi, and at the end of the experiment (35th dpi)^[17]. Small intestine

and muscle specimens were collected 7th and 35th dpi, respectively and were divided into two parts. One part was fixed in formalin 10% for further H&E staining and histopathological examination. The 2nd part was frozen at -80°C for the detection of *T. spiralis* larval DNA by real-time PCR.

Blood samples collection: Two ml blood, drawn from the submandibular vein in plain tubes, were allowed to clot, then centrifuged to separate the serum. The serum was stored at -20°C for subsequent immunological measurement of IgM, IgG1 and estimation of serum *T. spiralis* circulating larval antigen using ELISA.

Isolation and counting of *T. spiralis* adults: On the 7th dpi, adult worms were isolated and counted^[20] from the small intestine of all infected and treated subgroups (Ib1, IIa1, IIb1, IIc1, IId1, and IIe1). The reduction rate was calculated: [(mean number in the positive control group - mean number in the treatment group)/mean number in the control group] × 100%^[21].

Isolation and counting of *T. spiralis* larvae: On the 35th dpi, larvae from abdominal muscles from infected and treated subgroups (Ib2, IIa2, IIb2, IIc2, IId2, and IIe2) were isolated by artificial digestion of muscular tissue. The artificial gastric juice was prepared by adding 1% pepsin (weight/volume) and 1% concentrated HCL (volume/volume) in warm tap water. The mixture was incubated at 37°C for two hours under continuous agitation using an electric stirrer. The digested product was passed through a copper sieve (50 mesh/inch) to remove the coarse particles. The filtered fluid was passed through a sieve (200 mesh/inch) to collect

excysted larvae^[20]. Both dead larvae (coma-shaped and non-motile) and living larvae (coiled and motile) were counted under the microscope. The reduction rate was accordingly calculated: [(mean number in the control group - mean number in the treatment group)/ mean number in the control group] × 100%^[21].

Estimation of serum IgM and IgG1 levels by ELISA^[22]: *T. spiralis* crude antigen at 125 g/ml concentration was coated on Maxsorp 96-well microtitre plates overnight at 4°C in carbonate-bicarbonate buffer with a pH of 9.4. Plates were blocked for two hours at room temperature with 250 µl/well of 2% bovine serum albumin diluted in PBS, pH 7.2, and 0.05% Tween 20 (PBS/BSA/T-20). Sera were diluted 1:100 in PBS/T20, added to plates (100 µl/well), and left to incubate for one hour at room temperature. After washing, 100 µl/well of diluted anti-mouse IgM and IgG1 (1 mg/ml each; Southern Biotech, USA) in PBS/T20 (1:5000 for IgG1) were added for 90 min. Reaction developed by adding 100µl/well of p nitrophenyl phosphate substrate and incubation until appearance of yellow color. Using an ELISA reader (Bio-Rad, UK), the absorbance was read at 405 nm.

Estimation of serum *T. spiralis* antigen level by indirect ELISA^[23]: Polyclonal antibodies were produced by immunization of a rabbit with crude *Trichinella* antigen^[23]. Sandwich ELISA was performed by subsequent addition of the coated unlabeled antibodies (primary), tested mice serum and enzyme labeled polyclonal antibodies specific to the antigen. Addition of a suitable substrate resulted in hydrolysis, the degree of which was proportional to the amount of attached enzyme. Absorbance of *Trichinella* antigen was measured at 492 nm using an ELISA reader^[24] (Bio-Rad microplate reader Richmond, Ca).

Detection of *T. spiralis* larva DNA in intestinal and muscular tissue by real-time PCR^[25]: Genomic DNA was extracted from frozen tissues (intestinal and muscular) using JET™ Genomic DNA Purification Mini Kit (Thermo Scientific, EU/Lithuania). The study utilized a forward primer (5- CATGGTTAGGTGAGATATTG-CCTGC-3), and reverse primer (5-GGTCCTCC-TTCCAGAAGATCTACTTTG-3)^[25]. Fluorescence was measured in the green channel and data was collected at the extension step. Cycle threshold (Ct) values were individually calculated by internal software using a manual threshold setting of 0.2 and 'dynamic tube' and 'ignore first 10 cycles' functions were activated. Each run was followed by a melt-curve analysis to verify specificity and match amplicons with positive control melt curve peaks. The amount of larval DNA identified by real-time PCR was inversely correlated with the cycle threshold in muscle tissue.

Histopathological study^[26]: Small intestine and muscle specimens were fixed and processed at the Pathology Department, Faculty of Medicine, Menoufia University. Specimens were washed, dehydrated,

cleared in xylene, and embedded in paraffin blocks. Paraffin sections (5 µm thickness) were stained with H&E, then examined microscopically.

Statistical analysis: Using SPSS (20), IBM Corp. released in 2011 (IBM SPSS Statistics for Windows, Version 20.0, Armonk, New York), data were coded, tabulated, and analyzed. Quantitative type data were expressed as mean and standard deviation (SD). The comparison of quantitative variables between two groups was determined using the Mann-Whitney test. The difference between the two means of the two distinct groups was evaluated using Post Hoc Value. A statistically significant difference was considered when $P=0.05$ or lower.

Ethical consideration: The present research followed the international guidelines of using experimental animals. The study was approved by the Ethical Committee of the Faculty of Medicine, Menoufia University, Egypt (IRB;12/2020PARA35).

RESULTS

Intestinal adult count: Examination of mice scarified at 7th dpi revealed that the highest reduction rate in adult *T. spiralis* count of 88.83% was detected in GIle1 (treated by albendazole), followed by 69.29% for GIId1 (treated by nanoliposomes-*TsCB* with aluminum hydroxide), then 53.29% for GIlc1 (treated by *TsCB* with aluminum hydroxide), with significance difference ($P_{13}<0.001$) between GIlc1 and GIId1. In addition, both subgroups treated by nanoliposomes-*TsCB* alone or with adjuvant (GIId1, and GIlb1) showed a significant difference ($P_{11}<0.001$). The least reduction rate (31.97%) was found in GIIa1 (treated by *TsCB*) (Table 3).

Muscular larva count: The larval count in mice sacrificed on the 35th dpi showed that the highest reduction rate was 89.7% detected in GIId2 (treated by nanoliposome-*TsCB* with aluminum hydroxide), followed by 65.7% in GIlb2 (treated by nanoliposome-*TsCB*), then 60.1% in GIle2 (treated by albendazole) with a statistically significant difference ($P_{13}<0.001$) between GIlc2 and GIId2. In addition, both subgroups treated by nanoliposome-*TsCB* alone or with aluminum hydroxide (GIId2 and GIlb2) showed a significant difference ($P_{11}<0.001$). The lowest reduction rate of 21.5% was recorded in GIIa2 (treated by *TsCB*) (Table 4).

Estimation of IgM level: In the intestinal phase, results revealed that the highest IgM level (0.47 ± 0.06) was detected in GIId1 (treated by nanoliposome-*TsCB* with aluminum hydroxide), followed by GIlb1 (treated by nanoliposome-*TsCB*) with a level of 0.30 ± 0.07 . While the lowest level (0.25 ± 0.05) was detected in GIle1 (treated by albendazole), with a

Table 3. Comparison of *T. spiralis* adult count among treated mice groups (intestinal phase), sacrificed on the 7th dpi.

Groups No.=5/subgroups	Adult count		Reduction%	Statistical analysis	
	Mean ± SD	Median		ANOVA	P value
G1a1	--	--	--		
G1b1	78.8 ± 2.6	80.0	--		
G1Ia1	53.6 ± 2.1	54.0	31.97	F=1328.6	<0.001**
G1Ib1	36.8 ± 1.8	36.5	47.83		
G1Ic1	39.1 ± 2.4	38.5	53.29		
G1Id1	24.2 ± 1.9	23.5	69.29		
G1Ie1	8.8 ± 1.5	8.0	88.83		

Post Hoc test
P1 (G1b1, and G1Ia1) <0.001**; *P1* (G1b1 and G1Ib1) <0.001**; *P3* (G1b1 and G1Ic1) <0.001**;
P4 (G1b1 and G1Id1) <0.001**; *P5* (G1b1 and G1Ie1) <0.001**; *P6* G1Ia1 and G1Ic1 <0.001**;
P7 (G1Ia1 and G1Id1) <0.001**; *P8* (G1Ia1 and G1Ie1) <0.001**; *P9* (G1Ib1 and G1Ic1) <0.001**;
P10 (G1Ib1 and G1Ic1) =0.018*; *P11* (G1Ib1 and G1Id1) <0.001**; *P12* (G1Ib1 and G1Ie1) <0.001**;
P13 (G1Ic1 and G1Id1) <0.001**; *P14* (G1Ic1 and G1Ie1) <0.001**; *P15* (G1Id1 and G1Ie1) <0.001**.

G1a1: Control negative; **G1b1:** Control positive; **G1Ia1:** Treated by *TsCB*; **G1Ib1:** Treated by nanoliposome-*TsCB*; **G1Ic1:** Treated by *TsCB* with aluminum hydroxide; **G1Id1:** Treated by nanoliposome-*TsCB* with aluminum hydroxide; **G1Ie1:** Treated by albendazole (drug control); **F:** One way ANOVA test; *: Significant ($P < 0.05$); **: Significant ($P < 0.001$).

Table 4. Comparison of larval count among treated mice groups during the muscular phase, sacrificed on the 35th dpi.

Groups No.=5/subgroups	Larval count		Reduction%	Statistical analysis	
	Mean ± SD	Median		ANOVA	P value
G1a2	---	----	----		
G1b2	54568 ± 1065.8	54000	----		
G1Ia2	42854.2 ± 572.8	42748.5	21.5	F=7293.1	<0.001**
G1Ib2	18695.5 ± 261.7	18617	65.7		
G1Ic2	31771 ± 463.4	31785	41.8		
G1Id2	5616.8 ± 775.7	5617.5	89.7		
G1Ie2	21771 ± 463.4	21785	60.1		

Post Hoc test
P1 (G1b2, and G1Ia2) <0.001**; *P2* (G1b2 and G1Ib2): <0.001**; *P3* (G1b2 and G1Ic2) <0.001**;
P4 (G1b2 and G1Id2) <0.001**; *P5* (G1b2 and G1Ie2) <0.001**; *P6* (G1Ia2 and G1Ic2) <0.001**;
P7 (G1Ia2 and G1Id2) <0.001**; *P8* (G1Ia2 and G1Ie2) <0.001**; *P9* (G1Ib2 and G1Ic2) <0.001**;
P10 (G1Ib2 and G1Ic2) <0.001**; *P11* (G1Ib2 and G1Id2) <0.001**; *P12* (G1Ib2 and G1Ie2) <0.001**;
P13 (G1Ic2 and G1Id2) <0.001**; *P14* (G1Ic2 and G1Ie2) <0.001**; *P15* (G1Id2 and G1Ie2) <0.001**

G1a2: Control negative; **G1b2:** Control positive; **G1Ia2:** Treated by *TsCB*; **G1Ib2:** Treated by nanoliposome-*TsCB*; **G1Ic2:** Treated by *TsCB* with aluminum hydroxide; **G1Id2:** Treated by nanoliposome-*TsCB* with aluminum hydroxide; **G1Ie2:** Treated by albendazole (drug control); **F:** One way ANOVA test; *: Significant ($P < 0.05$); **: Significant ($P < 0.001$).

statistically significance difference between G1Id1 and G1Ie1 ($P_{15} < 0.001$). Similarly, there was a statistically significant difference between both groups treated by nanoliposome-*TsCB* alone or with aluminum hydroxide (G1Ib1 and G1Id1), respectively ($P_{11} < 0.001$) (Graph 1).

In the muscular phase, the highest IgM level (0.34±0.04) was found in G1Id2 (treated by nanoliposome-*TsCB* with aluminum hydroxide), followed by G1Ib2 (treated by nanoliposome-*TsCB*) with level the of 0.39±0.05. While, the lowest IgM level (0.25±0.02) was found in G1Ia2 (treated by *TsCB*), with a statistically significance difference between G1Id2 and G1Ia2 ($P_8 < 0.001$). There was also a significant difference between both groups treated with nanoliposome-*TsCB* alone or with aluminum hydroxide (G1Ib2, and G1Id2) ($P_{11} = 0.026$) (Graph 1).

Estimation of IgG1 level: In the intestinal phase, the results revealed highest level of IgG1 OD (0.29±0.03) in G1Id1 (treated by nanoliposome-*TsCB* with aluminum hydroxide), followed by G1Ib1 (treated by

nanoliposome-*TsCB*) with serum level 0.28±0.03. The lowest level (0.20±0.05) was recorded in G1Ia1 (treated by *TsCB*) with a statistically significance difference between the highest and lowest treated subgroups ($P_7 < 0.001$). There was also a statistically significant difference between both groups treated by nanoliposome-*TsCB* alone or with aluminum hydroxide (G1Ib1 and G1Id1) respectively ($P_{11} < 0.001$) (Graph 2).

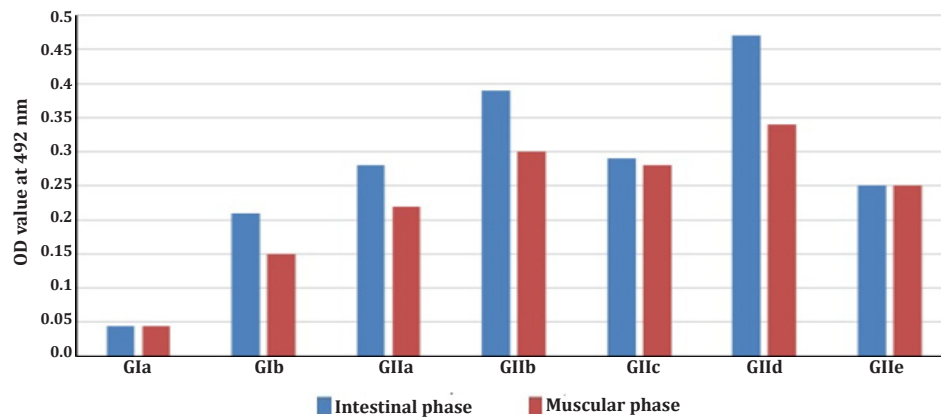
In the muscular phase, the highest IgG1 level (0.49±0.06) was detected in G1Id2 (treated by nanoliposome-*TsCB* with aluminum hydroxide), followed by G1Ib2 (treated by nanoliposome-*TsCB*) with serum level 0.46±0.03. The least IgM level (0.23±0.05) was recorded in G1Ie2 treated by albendazole, with a statistically significance difference between the highest and lowest treated groups ($P_{15} < 0.001$). There was also a statistically significant difference between both groups treated by liposome-*TsCB* alone or with aluminum hydroxide (G1Ib2, and G1Id2) ($P_{11} < 0.001$) (Graph 2).

Estimation of *T. spiralis* circulating larval antigen level: In the intestinal phase, the lowest level (0.56 ± 0.04) was found in GIId1 (treated by nanoliposome-*TsCB* with aluminum hydroxide, and GIId1 (treated by nanoliposome-*TsCB*), while the highest level (0.85 ± 0.040) was detected in GIId1 (treated by albendazole) then GIIa1 (treated by *TsCB*) (0.78 ± 0.06). There was no statistically significant difference between both groups treated by nanoliposome-*TsCB* alone or with aluminum hydroxide (GIId1 and GIId1 respectively) (Graph 3).

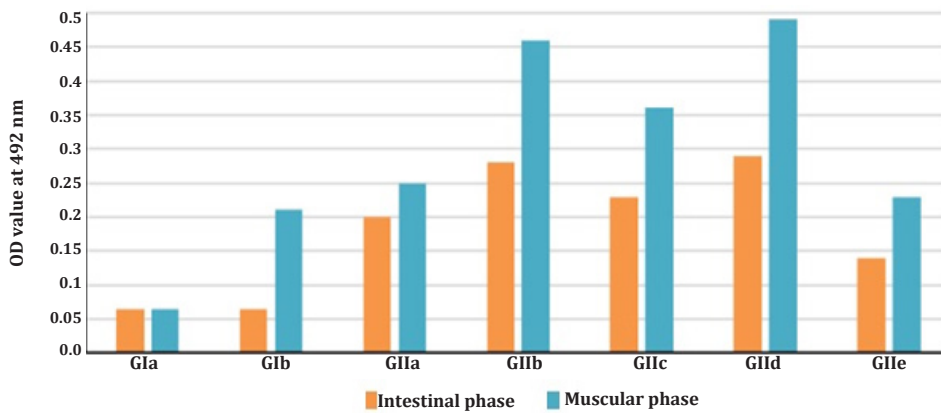
In the muscular phase, the lowest antigen level (0.76 ± 0.04) was detected in GIId2 (treated by nanoliposome-*TsCB* with aluminum hydroxide)

followed by (0.84 ± 0.04) in GIId2 (treated by nanoliposome-*TsCB*), while the highest antigen level (1.42 ± 0.41) was found in GIIa2 (treated by *TsCB*) followed by 1.1 ± 0.06 in GIId2 (treated by *TsCB* with aluminum hydroxide). While there is no statistically significant difference between both groups treated by nanoliposome-*TsCB* alone or with aluminum hydroxide (GIId2 and GIId2) (Graph 3).

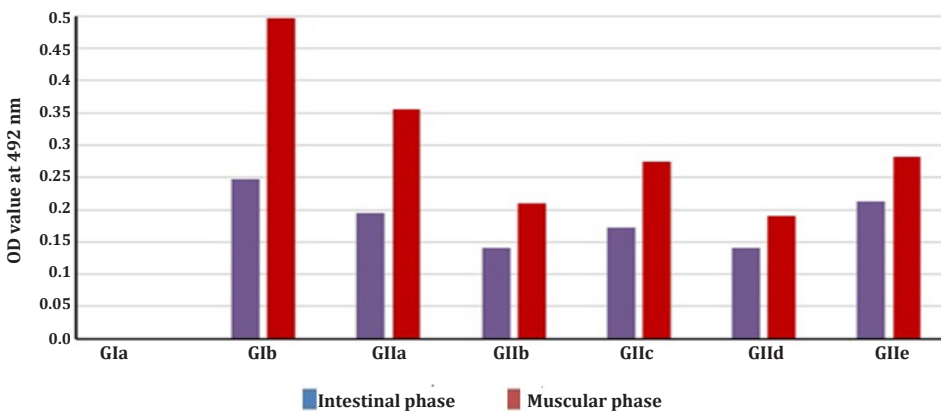
Real time PCR: In the intestinal phase, the lowest value of cycle threshold (30.26 ± 0.28) was in GIId1 (treated by albendazole), followed by GIId1 (treated by *TsCB* with aluminum hydroxide) (30.54 ± 0.4), then GIIa1 (treated by *TsCB*) (30.59 ± 0.3). The highest value (32.9 ± 0.23) was detected in GIId1 (treated by nanoliposome-



Graph 1. IgM level in intestinal and muscular phases (7th and 35th dpi respectively).



Graph 2. IgG level in intestinal and muscular phases (7th and 35th dpi respectively).



Graph 3. *T. spiralis* circulating larval antigen level in intestinal and muscular phases (7th and 35th dpi respectively).

TsCB with aluminum hydroxide), followed by GIb1 (treated by nanoliposome-TsCB) (31.76±0.22). There was no statically significant difference between both groups treated by nanoliposome-TsCB with or without aluminum hydroxide (GIb1 and GIId1 respectively), as well as between GIb1 and GIle1 and GIc1 and GIle1, respectively (Table 5).

In the muscular phase, the lowest value of cycle threshold was 29.93±0.49 in GIIa2 (treated by TsCB), followed by GIc2 (treated by TsCB with aluminum hydroxide) (30.31±0.399), while the highest value was 32.1±0.62 in GIId2 (treated by nanoliposome-TsCB with aluminum hydroxide). followed by (31.76±0.22) in GIb2 (treated by nanoliposome-TsCB). Furthermore, there was no statically significant difference between both groups treated by nanoliposome-TsCB with or without aluminum hydroxide (Table 6).

Histopathological examination: In the intestinal phase, GIa1 control negative mice showed normal intestinal tissue with preserved villous /crypt ratio, and no inflammation (Fig. 1a); while in infected untreated subgroup (GIb1), there was severe inflammation, dense inflammatory infiltrate in lamina propria, edema, destruction of intestinal villi and ulceration (Fig. 1b, c). Moderate destruction and moderate inflammation with mild eosinophilic inflammatory infiltrate was detected in GIIa1 (treated by TsCB) (Fig. 1d). Moreover, subgroup GIb1 (treated by nanoliposome-TsCB) showed mild decrease in villous/crypt ratio with mild inflammatory cells, and mild edema (Fig. 1e). Subgroup GIc1 (treated by TsCB with aluminum hydroxide) showed preserved villous/crypt ratio and mild crypt hyperplasia, focal blunting of villi, mild inflammation, and mild edema (Fig. 1f). There was marked improvement of inflammation with lowest intensity of destruction,

Table 5. Comparison between the cycle threshold values of RT-PCR among treated groups in the intestinal phase (7th dpi).

Groups No.=5/subgroups	Adult count		Range	Statistical analysis	
	Mean ± SD	Median		ANOVA	P value
GIa1	----	----	----		
GIb1	24.44 ± 0.96	24.8	23.0 - 25.65		
GIIa1	30.59 ± 0.3	30.535	30.2 - 31.0		
GIb1	31.76 ± 0.22	31.845	31.4 - 32.0	F=379.292	<0.001**
GIc1	30.54 ± 0.4	30.6	29.9 - 30.6		
GIId1	32.9 ± 0.23	32.9	32.45 - 33.24		
GIle1	30.26 ± 0.28	30.18	29.9 - 30.7		

Post Hoc test P1 (GIb1 and GIIa1) <0.001**; P2 (GIb1 and GIb1); <0.001**; P3 (GIb1 and GIc1) <0.001**;
 P4 (GIb1 and GIId1); <0.001**; P5 (GIb1 and GIle1) <0.001**; P6 (GIIa1 and GIc1) <0.001**;
 P7 (GIIa1 and GIId1) =0.811; P8 (GIIa1 and GIle1) <0.001**; P9 (GIb1 and GIc1)=0.106;
 P10 (GIb1 and GIc1) <0.001**; P11 (GIb1 and GIId1) =.874; P12 (GIb1 and GIle1) =0.168;
 P13 (GIc1 and GIId1) <0.001**; P14 (GIc1 and GIle1) =0.168; P15 (GIId1 and GIle1) <0.001**

GIa1: Control negative; **GIb1:** Control positive; **GIIa1:** Treated by TsCB; **GIb1:** Treated by nanoliposome-TsCB; **GIc1:** Treated by TsCB with aluminum hydroxide; **GIId1:** Treated by nanoliposome-TsCB with aluminum hydroxide; **GIle1:** Treated by albendazole (drug control); **F:** One way ANOVA test; *: Significant (P<0.05); **: Significant (P <0.001).

N.B.: Cycle threshold is indirectly proportional to the amount of larval DNA detected by real-time PCR.

Table 6. Comparison between the cycle threshold values of RT-PCR among treated groups in the muscular phase (35th dpi).

Groups No.=5/subgroups	Larval count		Range	Statistical analysis	
	Mean ± SD	Median		ANOVA	P value
GIa2	----	----	----		
GIb2	24.95±1.29	25.87	23.0 - 26.0		
GIIa2	29.93±0.49	30.34	29.34 - 30.6		
GIb2	31.66±0.68	30.9	30.9 - 32.9	F=119.077	<0.001**
GIc2	30.31±0.399	30.15	29.9 - 31.1		
GIId2	32.1±0.62	31.9	31.45 - 33.24		
GIle2	30.35±0.85	30.05	29.47 - 31.98		

Post Hoc test P1 (GIb2 and GIIa2) <0.001**; P2 (GIb2 and GIb2) <0.001**; P3 (GIb2 and GIc2) <0.001**;
 P4 (GIb2 and GIId2) <0.001**; P5 (GIb2 and GIle2) =0.011*; P6 (GIIa2 and GIc2) =0.972;
 P7 (GIIa2 and GIId2) <0.001**; P8 (GIIa2 and GIle2)=0.653 ; P9 (GIb2 and GIc2) <0.1*;
 P10 (GIb2 and GIc2) <0.001**; P11 (GIb2 and GIId2) =0.035*; P12 (GIb2 and GIle2) <0.001** ;
 P13 (GIc2 and GIId2) <0.001**; P14 (GIc2 and GIle2) <0.001**; P15 (GIId2 and GIle2) <0.001**

GIa2: Control negative; **GIb2:** Control positive; **GIIa2:** Treated by TsCB; **GIb2:** Treated by nanoliposome-TsCB; **GIc2:** Treated by TsCB with aluminum hydroxide; **GIId2:** Treated by nanoliposome-TsCB with aluminum hydroxide; **GIle2:** Treated by albendazole (drug control); **F:** One way ANOVA test; *: Significant (P<0.05); **: Significant (P <0.001).

N.B.: Cycle threshold is indirectly proportional to the amount of larval DNA detected by real-time PCR.

minimal eosinophilic infiltrate and minimal affection of intestinal villi and crypt (in subgroup GIId1 (treated by nanoliposome-*TsCB* with aluminum hydroxide) (Fig. 1g). Furthermore, the albendazole treated group (GIIe1), showed mild degree of inflammation (Fig. 1h).

Concerning the muscular phase, the non-infected control group (GIIa2) showed normal muscle without inflammation and absence of larvae (Fig. 2a), while there was a dense larval deposition in infected control group (GIIb2), each surrounded by a thick intact capsule with intense inflammatory infiltrate consisting mainly of lymphocytes and macrophages with fat deposition (Fig. 2b and c). There was a moderate density of encysted *T. spiralis* larvae associated with moderate inflammation, moderate fragmentation of internal

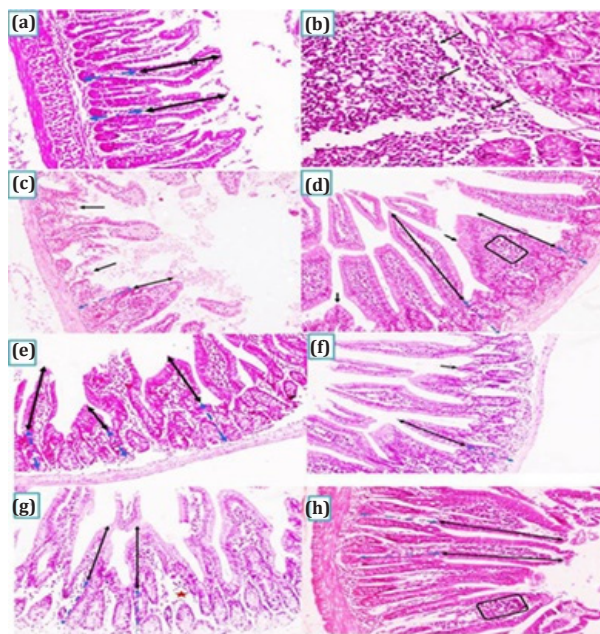


Fig. 1. TS histopathology of intestinal tissues. **(a)** GIa1 (control negative) showed preserved villous (continuous black arrows)/crypt (interrupted blue arrows) ratio and no inflammation (H&E x40); **(b)** GIb1 (control positive) showed dense inflammation with lymphoid aggregates (black arrows) (H&E x100); **(c)** The same group showed marked blunting of villi (black short arrows), a decrease in villous (black arrows)/ crypt (blue arrows) ratio, and moderate edema (H&E x40); **(d)** GIla1 (treated by *TsCB*) showed preserved villous/crypt ratio (black and blue arrows) and mild blunting of villi (short black arrow), moderate inflammation (box), and mild edema (H&E x40); **(e)** GIlb1 (treated by nanoliposome-*TsCB*) showed a mild decrease in villous (black arrow)/crypt (blue arrow) ratio with mild inflammatory cells, and mild edema (H&E x40); **(f)** GIlc1 (treated by *TsCB* with aluminum hydroxide) showed a preserved villous/crypt ratio (black arrows) and mild crypt hyperplasia (blue arrows), focal blunting of villi (short black arrow), mild inflammation, and mild edema (H&E x40); **(g)** GIId1 (treated by nanoliposome-*TsCB* with aluminum hydroxide) showed a mild decrease in villous/crypt ratio (black arrows) and mild crypt hyperplasia (blue arrows), mild inflammation, and moderate edema (asterisk) (H&E x40); **(h)** GIIe1 (treated by albendazole) group showed a preserved villous/crypt ratio (black arrows) and mild crypt hyperplasia (blue arrows), mild inflammation, and mild edema (H&E x40).

structures in subgroup GIla2 group (treated by *TsCB*) (Fig. 2d). Moreover, the group treated by nanoliposome-*TsCB* (GIIb2) showed moderate inflammatory cellular infiltration and mild muscle degradation (Fig. 2e). In GIlc2 group (treated by *TsCB* with aluminum hydroxide), there were encysted *T. spiralis* larvae associated with little inflammation, moderate fragmentation of internal structures and moderate degeneration of surrounding muscle (Fig. 2f). The lowest intensity of larval deposition and larval degeneration in the form of fragmentation, vacuolation and homogenization were noticed in subgroup GIId2 (treated by nanoliposome-*TsCB* with aluminum hydroxide). It also showed mild inflammatory cellular infiltration, mild muscle

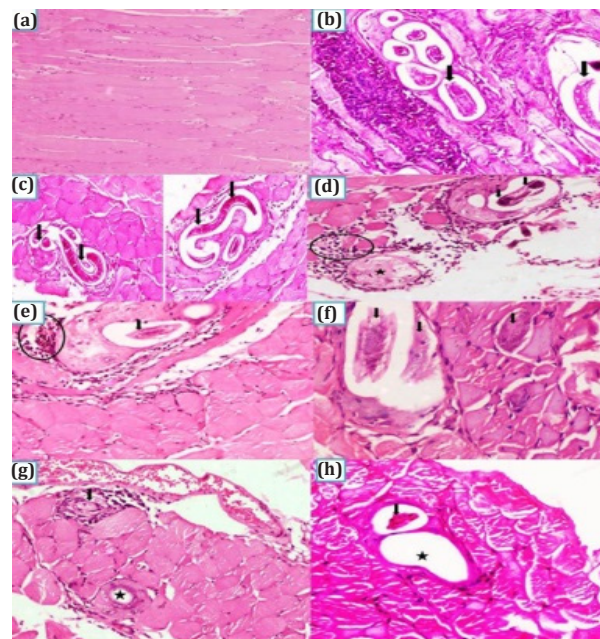


Fig. 2. TS histopathology of muscle tissues. **(a)** GIa2 (non-infected control group) showed normal muscle with little inflammation and no larvae (H&E x100); **(b)** GIb2 (infected control) showed a large density of encysted *T. spiralis* larvae associated with marked inflammation and mild fragmentation of internal structures (black arrows) (H&E x200); **(c)** GIb2 (infected control) showed encysted *T. spiralis* larvae with mild fragmentation of internal structures (black arrows) (H&E x100); **(d)** GIla2 group (treated with *TsCB*) showed moderate density of encysted *T. spiralis* larvae associated with moderate inflammation, moderate fragmentation of internal structures (black arrows), with occasional empty larvae (asterisk) and mild degeneration of surrounding muscle (H&E x200); **(e)** GIlb2 group (treated by nanoliposome-*TsCB*) showed encysted *T. spiralis* larvae associated with moderate inflammation (circle), marked fragmentation of internal structures (black arrow), and mild degeneration of surrounding muscle (H&E x400); **(f)** GIlc2 group (treated by *TsCB* with aluminum hydroxide) showed encysted *T. spiralis* larvae associated with little inflammation, moderate fragmentation of internal structures (black arrows), and moderate degeneration of surrounding muscle (H&E x400); **(g)** GIId2 group (treated by nanoliposome-*TsCB* with aluminum hydroxide) showed encysted *T. spiralis* larvae associated with mild inflammation, marked fragmentation of internal structures (black arrows) with empty larvae (asterisk), and mild degeneration of surrounding muscle (H&E x100); **(h)** GIIe2 group (treated by albendazole) showed encysted *T. spiralis* larvae associated with little inflammation, marked fragmentation of internal structures (black arrows) with empty larvae (asterisk), and moderate degeneration of surrounding muscle (H&E x200).

degradation and the highest degree of muscle capsule thinning (Fig. 2g). Furthermore, the highest intensity of larval deposition and severe muscle degradation were detected in GIIe2 (treated by albendazole) (Fig. 2h).

DISCUSSION

Trichinosis is a zoonotic disease with a worldwide distribution caused by *T. spiralis* acquired through the ingestion of undercooked meat of infected animals. Effective medications are limited due to their side effects and resistance, so there is a need for developing safe and effective drugs^[27]. Cysteine proteases are essential for compromising the integrity of the gut epithelium and facilitating the invasion, development, and survival of larvae in hosts. Therefore, *T. spiralis* cysteine proteases may be considered the primary prospective target molecules for therapy against larval invasion and development^[28]. Key functions in parasite survival, host invasion, and host immune response are played by secretory cathepsin B protease, a significant papain-like cysteine protease^[6]. Using nanoliposome vesicles to deliver common anti-parasitic medications has increased their effectiveness due to their synergistic effects without appearing to be detrimental to the host cells^[29].

Regarding adult *T. spiralis* number, our results are in harmony with Cui *et al.*^[30] who postulated that vaccinated mice with *TsCB* resulted in 52.81% adult worm burden reduction and 50.90% muscle larvae burden reduction. Thus, the *TsCB*-specific antibody response apparently impeded intestinal worm growth and decreased the female fecundity. In addition, Hassan *et al.*^[31] reported that relative to the control group, there was a 93.1% decrease in worm counts and 90.3%, 79.5% reductions in hepatic and intestinal egg burdens, respectively in vaccinated mice with cathepsin B against *S. mansoni*. Besides, Buffoni *et al.*^[32] and Villa-Mancera *et al.*^[33] evaluated the effect of vaccination with cathepsin on *Fasciola* infected animals and demonstrated a considerable decrease in size, net weight, and egg production by the fluke.

Furthermore, several other studies on experimental trichinosis using different nanoparticles alone or in a combination with other drugs gave similar results. For example, Hassan *et al.*^[34] reported a significant reduction (93.3%) of the adult worms of *T. spiralis* in the small intestine in the group treated with ivermectin combined with nitazoxanide loaded on solid lipid nanoparticles (NTZ-SLNs). Also, the count of encysted larvae in muscles was highly decreased in the NTZ-SLNs group (89% reduction rate). In addition, Nassef *et al.*^[35,36] reported that chitosan nanoparticles loaded with a full dose of albendazole gave a high reduction percentage in numbers of *T. spiralis* adults and larvae (99% and 97.3% respectively).

Results of IgM and IgG1 levels coincide with Yang *et al.*^[6] findings in which they demonstrated the remarkable antigenicity of r*TsCB* to stimulate robust IgG. The latter in turn activates Th2 cytokines thus indicating the possible use as an immunomodulatory drug. Moreover, good antigenicity and high protection are produced by *TsCB* by boosting anti-*Trichinella* antibodies, particularly in the intestinal stage, which is crucial for infection control. Accordingly, *TsCB* may be proposed as a promising therapy for control of trichinosis^[30]. Besides, two studies^[2,37] reported that vaccinated mice with recombinant *T. spiralis* serine proteinase (r*TsSP*) caused elevation in serum anti-r*TsSP*-specific IgG titers, indicating that the r*TsSP* was strongly immunogenic.

Furthermore, it was reported that vaccination with cathepsin plus adjuvant (Montanide or AddaVax) against *S. mansoni*, elicited a higher mixed IgG1/IgG2 response, and the vaccinated group with CB against the same parasite had significantly higher anti-CB IgG1 titers^[38,39], respectively. On the other hand, two studies^[34,40] reported that there was no statistically significant difference in anti-*T. spiralis* IgG level between all groups before and after treatment with albendazole and ivermectin combined with NTZ-SLNs, respectively. This may be due to using solid lipid nanoparticles. But in our current study, the liposome nanoparticles used, effected the Th2 cells inducing elevation of its cytokines and stimulating antibodies production by B cells.

In the current work, *T. spiralis* circulating larval antigen level was decreased after treatment in all groups with the highest reduction in groups treated by nano-CB and nano-CB with aluminum hydroxide. Our recorded results concerning the circulating larval antigen coordinated with Zhan *et al.*^[39] who reported that the levels of circulating antigen (CAg) in the albendazole-treated group decreased gradually, and by 28th day after treatment the CAg levels decreased to the control level.

Additionally, results of real time PCR agreed with observations of Cuttell *et al.*^[25] who used the same primers to measure cycle threshold in mice infected with *T. spiralis*. Furthermore, Al-Attar *et al.*^[41] reported that the amount of larval DNA in the muscle tissues of all groups that received treatment decreased after treatment with adult and larval E/S antigens.

The recorded histopathological changes of the intestinal tissue in our study coincided with Liu *et al.*^[42] report and postulation that r*TsCB* is effective in ameliorating intestinal injury and improving intestinal function. It mediates this efficacy by switching immunity from M2 to M1 macrophages. So, r*TsCB* may provide potential therapeutic effects. Furthermore, these results were in accordance with Nassef *et al.*^[36] and Hassan *et al.*^[34] who reported similar results

using chitosan nanoparticles loaded with a full dose of albendazole and ivermectin with NTZ-SLNs respectively.

Our results concerning the histopathological changes of the muscular tissue are in parallel with Lu *et al.*^[43], they showed that polysaccharide nanocarrier expressing *T. spiralis* cathepsin F vaccine alone can considerably reduce the number of larvae encapsulated in muscles, the load of adult worms, and intestinal pathological damage. Moreover, several studies^[44-46] used different nanoparticles alone or in combination with other drugs and reported improvement of the pathological and inflammatory changes induced by *T. spiralis* in the infected mice. This was attributed to the increased solubility, bioavailability, and efficiency of nanoparticles.

In the present work, nano-liposome-TsCB gave the best therapeutic result among all treated subgroups in all assessment parameters. Nanoparticles have therapeutic and protective effects as they possess special characters. Liposomes result in a net positive charge for improved medication uptake by cells. However, liposomes alone exhibit substantial immune-modulating antiparasitic action. Additionally, the liposome has great capacity to block several stages of the parasite life cycle and has an equal impact on drug-sensitive and drug-resistant parasites^[29]. Furthermore, the administration of CB as therapy, generates anti-rTsCB antibodies that impede partially the larval intrusion of enterocytes and maintains the therapeutic effect; this is because cathepsin facilitates the larval invasion of intestinal epithelium^[4].

In the current study, using aluminum hydroxide as adjuvant improved the efficacy of TsCB and nano-TsCB in all assessment parameters against trichinellosis. In particular eosinophils, Th2-type cells, appear to respond well to aluminum adjuvants. Aluminum draws eosinophils via encouraging mast cell-dependent IL-5 production, just like helminth eggs do. Additionally, the release of IL-12 by dendritic cells is inhibited by aluminum adjuvants like aluminum hydroxide and aluminum phosphate^[47].

In conclusion, our study showed that *T. spiralis* CB and nano-liposomes CB antigens have therapeutic effects on experimental trichinosis by decreasing adult and larval numbers and enhancing the pathological alterations in both the intestinal and muscle tissues. It also caused a significant increase in serum IgM and IgG1 levels, decreased *T. spiralis* circulating larval antigen levels, and increased the mean cycle threshold values of intestinal and muscular tissues (decreased larval DNA). Using nano-liposome CB enhanced the results in all parameters, using aluminum hydroxide as an adjuvant also improved the efficacy of TsCB and nano-liposome TsCB.

Author contributions: Atia AF, EL-Kersh WM, El-Nahas NS, Moharm IM, Lasheen ME and Abo-Hussien NM conceived and designed the research topic. Atia AF, Abo-Hussien NM and Lasheen ME were responsible for acquisition, analysis and interpretation of the research data. Lasheen ME wrote the draft of the manuscript. Atia AF, EL-Kersh WM, El-Nahas NS, Moharm IM and Abo-Hussien NM critically revised the article for publication. All the authors approved the final revision before publication.

Conflict of Interest: The authors affirm that they have no financial or other conflicts of interest.

Funding statement: No specific grant for this research was provided by funding organizations in the public, private, or nonprofit sectors.

REFERENCES

1. Yayah M, Yadesa G, Erara M, Fantahun S, Gebru A, Birhan M. Epidemiology, diagnosis, and public health importance of trichinellosis. *Online J Anim Feed Res* 2020; 10.3:131-139.
2. Sun GG, Lei JJ, Ren HN, Zhang Y, Guo KX, Long S, *et al.* Intranasal immunization with recombinant *Trichinella spiralis* serine protease elicits protective immunity in BALB/c mice. *Exp Parasitol* 2019; 201:1-10.
3. Saracino MP, Calcagno MA, Beauche EB, Garnier A, Vila CC, Granchetti H *et al.* *Trichinella spiralis* infection and transplacental passage in human pregnancy. *Vet Parasitol* 2016; 231:2-7.
4. Han Y, Yue X, Hu CX, Liu F, Liu RD, He M, *et al.* Interaction of a *Trichinella spiralis* cathepsin B with enterocytes promotes the larval intrusion into the cells. *Res Vet Sci* 2020; 130:110-117.
5. Liu RD, Qi X, Sun GG, Jiang P, Zhang X, Wang L, *et al.* Proteomic analysis of *Trichinella spiralis* adult worm excretory-secretory proteins recognized by early infection sera. *Vet Parasitol* 2016; 231:43-46.
6. Yang Z, Li W, Yang Z, Pan A, Liao W, Zhou X. A novel antigenic cathepsin B protease induces protective immunity in *Trichinella*-infected mice. *Vaccine* 2018; 36(2):248-255.
7. Jeevanandam J, Barhoum A, Chan YS, Dufresne A, Danquah MK. Review on nanoparticles and nanostructured materials: History, sources, toxicity, and regulations. *Beilstein J Nanotechnol* 2018; 9:1050-1074.
8. Su S, Kang P. Recent advances in nanocarrier-assisted therapeutics delivery systems. *Pharmaceutics* 2020; 12(9): 837.
9. Zarrabi A, Alipoor AM, Khorasani S, Mohammadabadi MR, Jamshidi A, Torkaman S, *et al.* Nanoliposomes and tocopherols as multifunctional nanocarriers for the encapsulation of nutraceutical and dietary molecules. *Molecules (Basel, Switzerland)* 2020; 25(3):638.
10. Aguilar-Pérez KM, Avilés-Castrillo JI, Medina DI, Parra-Saldivar R, Iqbal HMN. Insight into nanoliposomes as smart nanocarriers for greening the twenty-first century biomedical settings. *Front Bioeng Biotechnol* 2020; 8: 579536.

11. Zamani P, Momtazi-Borojeni AA, Nik ME, Oskuee RK, Sahebka A. Nanoliposomes as the adjuvant delivery systems in cancer immunotherapy. *J Cell Physiol* 2018; 233:5189–5199.
12. Zhang N, Li W, Fu B. Vaccines against *Trichinella spiralis*: Progress, challenges, and future prospects. *Transbound Emerg Dis* 2018; 65: 1447- 1458.
13. Kołodziej-Sobocińska M, Dvorožňaková E, Dziemian E. *Trichinella spiralis*: Macrophage activity and antibody response in chronic murine infection. *Exp Parasitol* 2006; 112: 52–62.
14. Ding J, Bai X, Wang X, Shi H, Cai X, Luo X, *et al.* Immune cell responses and cytokine profile in intestines of mice infected with *Trichinella spiralis*. *Front Microbiol* 2017; 8: 2069.
15. Smith AM, Dowd AJ, McGonigle S, Keegan PS, Brennan G, Trudgett A, *et al.* Purification of a cathepsin L-like proteinase secreted by adult *Fasciola hepatica*. *Mol Biochem Parasitol* 1993; 62(1): 1-8.
16. Di Pasqua AJ, Mishler RE, Ship YL, Dabrowiak JC, Asefa T. Preparation of antibody-conjugated gold nanoparticles. *Mater Lett* 2009; 63(21): 1876-1879.
17. Nasreldin N, Swilam S, Abd-Elrahman SM, Abd El-ghaffar SK. Evaluation of clinicopathological alterations in mice experimentally infected with *Trichinella spiralis* and the nematocidal effect of tannic acid and albendazole. *NVVJ* 2022; 2(1), 16-27.
18. Lindblad EB. Aluminum compounds for use in vaccines. *Immunol Cell Biol* 2004; 82:497–505.
19. Bakir HY, Attia RA, Mahmoud AE, Ibraheim Z. M-RNA gene expression of INF- γ and IL-10 during intestinal phase of *Trichinella spiralis* after Myrrh and Albendazole treatment. *Iran J Parasitol* 2017; 12 (2):188-195.
20. Quan FS, Bae JS, Lee JB, Min YK, Yang HM, Joo K, *et al.* Protective immunity against challenge infection with *Trichinella spiralis* in the rat. *Acta Med* 2008; 52:101-106.
21. Saad AE, Ashour DS, Abou-Rayia DM, Bedeer AE. Carbonic anhydrase enzyme as a potential therapeutic target for experimental trichinellosis. *Parasitol Res* 2016; 115:2331–2339.
22. Nöckler K, Reckinger S, Broglia A, Mayer-Scholl A, Bahn P. Evaluation of a Western Blot and ELISA for the detection of anti-*Trichinella*-IgG in pig sera. *Vet Parasitol* 2009; 163(4):341-347.
23. Abdel-Megeed KN, Abdel-Rahman EH. *Fasciola gigantica*, immunization of rabbits with proteins isolated from coproantigen. *J Egypt Soc Parasitol* 2004; 34:631-642.
24. Liu LN, Jing FJ, Cui J, Fu GY, Wang Z Q. Detection of circulating antigen in serum of mice infected with *Trichinella spiralis* by an IgY-IgM mAb sandwich ELISA. *Exp Parasitol* 2013; 133(2):150–155.
25. Cuttall L, Corleya SW, Graya CP, Vander-lindeb PB, Jackson LA, Traub J, *et al.* Real-time PCR as a surveillance tool for the detection of *Trichinella* infection in muscle samples from wildlife. *Vet Parasitol* 2012; 188:1-9
26. Drury RB, Wallington EA. Carleton,s Histological Technique. UK: Oxford University Press 1980; 4th ed: 250.
27. El-Kady AM, Abdel-Rahman IAM, Sayed E, Wakid MH, Alobaid HM, Mohamed KH, *et al.* A potential herbal therapeutic for trichinellosis. *Front Vet Sci* 2022; 9, 970327.
28. Song YY, Lu QQ, Han LL, Yan SW, Zhang XZ, Liu R, *et al.* Proteases secreted by *Trichinella spiralis* intestinal infective larvae damage the junctions of the intestinal epithelial cell monolayer and mediate larval invasion. *Vet Res* 2022; 53(1):19.
29. Vassoudevane J, Mariebernard M, Rajendran V. Stearylamine liposome as an anti-parasitic agent. *Drugs Drug Candidates* 2023; 2(1):95-108.
30. Cui J, Han Y, Yue X, Liu F, Song Y, Yan S, *et al.* Vaccination of mice with a recombinant novel cathepsin B inhibits *Trichinella spiralis* development, reduces the fecundity and worm burden. *Parasit Vectors* 2019; 12:1-12.
31. Hassan AS, Zelt NH, Perera DJ, Ndao M, Ward BJ. Vaccination against the digestive enzyme cathepsin B using a YS1646 *Salmonella enterica* Typhimurium vector provides almost complete protection against *Schistosoma mansoni* challenge in a mouse model. *PLoS Neg Trop Dis* 2019; 13(12): e0007490.
32. Buffoni L, Garza-Cuartero L, Pérez-Caballero R, Zafra R, Javier Martínez-Moreno F, Molina-Hernández V, *et al.* Identification of protective peptides of *Fasciola hepatica*-derived cathepsin L1 (FhCL1) in vaccinated sheep by a linear B-cell epitope mapping approach. *Parasit Vectors* 2020; 13(1):1-13.
33. Villa-Mancera A, Olivares-Pérez J, Olmedo-Juárez A, Reynoso-Palomar A. Phage display-based vaccine with cathepsin L and excretory-secretory products mimotopes of *Fasciola hepatica* induces protective cellular and humoral immune responses in sheep. *Vet Parasitol* 2021; 289:109340.
34. Hassan MM, El-Rahman A, Abd El-Hamed E, Abdel Fattah A, Harb O, Mohamed S, *et al.* The impact of nitazoxanide loaded on solid lipid nanoparticles on experimental trichinellosis. *Zagazig Univ Med J (ZUMJ)* 2021; 27(6):1074-1084.
35. Nassef NE, Moharm IM, Atia AF, Brakat RM, Abo-Hussien NM, Mohamed A. Therapeutic efficacy of chitosan nanoparticles and albendazole in intestinal murine trichinellosis. *J Egypt Soc Parasitol* 2018; 48(3):493-502.
36. Nassef NE, Moharm IM, Atia AF, Brakat RM, Abo-Hussien NM, Shamseldeen A. Therapeutic efficacy of chitosan nanoparticles loaded with albendazole on parenteral phase of experimental trichinellosis. *J Egypt Soc Parasitol* 2019; 49(2):301-311.
37. Jin QW, Zhang N Z, Li WH, Qin HT, Liu YJ, Ohiolei JA, *et al.* *Trichinella spiralis* thioredoxin peroxidase2 regulates protective Th2 immune response in mice by directly inducing alternatively activated macrophages. *Front Immunol* 2020; 11:2015.
38. Perera DJ, Hassan AS, Jia Y, Ricciardi A, McCluskie MJ, Weeratna R, *et al.* Adjuvanted *Schistosoma mansoni*-cathepsin B with sulfated Lactosyl Archaeol Archaeosomes or AddaVax™ provides protection in a pre-clinical schistosomiasis model. *Front Immunol* 2020; 11:605288.
39. Hassan AS, Houle S, Labrie L, Perera DJ, Dozois CM, Ward B, *et al.* *Salmonella Typhimurium* expressing chromosomally integrated *Schistosoma mansoni* cathepsin B protects

- against schistosomiasis in mice. NPJ Vaccines 2023; 8(1):27.
40. Zhan JH, Yao JP, Liu W, Hu XC, Wu ZD, Zhou X. Analysis of a novel cathepsin B circulating antigen and its response to drug treatment in *Trichinella*-infected mice. Parasitol Res 2013; 112:3213-3222.
41. Al-Attar TA, El-Kersh WM, Sadek GS, Harba N, Osheiba SF, Brakat R. A study of immunotherapeutic efficacy of *Trichinella spiralis* excretory-secretory proteins in murine trichinellosis. J Egypt Soc Parasitol 2020; 50(2):281-292.
42. Liu WF, Wen SH, Zhan JH, Li YS, Shen JT, Yang W, *et al.* Treatment with recombinant *Trichinella spiralis* cathepsin B-like protein ameliorates intestinal ischemia/reperfusion injury in mice by promoting a switch from M1 to M2 macrophages. J Immunol 2015; 195(1):317-328.
43. Lu H, Wang Y, Zhang T, Quan Y, Zhu Z, Xue Y, *et al.* *Lycium barbarum* polysaccharide promotes the immunoprotective effects of recombinant *Lactobacillus plantarum* vaccine expressing *Trichinella spiralis* cathepsin F-like protease1 gene. Research Square 2023; <https://europepmc.org/article/ppr/ppr620884>.
44. Atia AF, Abokhalil NA, Sweed DM, Moaz IM, Abo-Hussien NM. Curcumin nanoparticles versus curcumin in amelioration of inflammatory and pathological changes during the migratory phase of murine trichinellosis. J Egypt Soc Parasitol 2021; 51(2):239-256.
45. Taha NM, Abdel-Radi Sh, Youssef FS, Auda HM, El-Bahy MM, Ramadan R. Parasiticidal efficacy of a new formulation of silver nanoparticles on *Trichinella spiralis* *in vitro*. J Adv Vet Res 2022; 12(4):379-385.
46. Khalifa MM, Ramadan RM, Youssef F, Auda HM, El-Bahy MM, Taha NM. Trichinocidal activity of a novel formulation of curcumin-olive oil nanocomposite *in vitro*. Vet Parasitol Reg Stud Reports 2023; 41:100880.
47. Terhune TD, Deth RC. Aluminum adjuvant-containing vaccines in the context of the hygiene hypothesis: A risk factor for eosinophilia and allergy in a genetically susceptible subpopulation? Int J Environ Health Res 2018; 15(5): 901.